Int J Thermophys (2009) 30:1975–1991
DOI 10.1007/s10765-009-0669-0

# Genetic Algorithm-Based Method for Determination of Temperature-Dependent Thermophysical Properties

**Balázs Czél · Gyula Gróf**

Received: 15 October 2008 / Accepted: 18 October 2009 / Published online: 10 November 2009


**Abstract** A new evaluation method based on a genetic algorithm is applied for simultaneous determination of the temperature-dependent thermal conductivity and volumetric heat capacity from transient temperature measurement data at two points according to the cooling down process of a three-layered infinite cylinder. Three test cases are presented defined with the consideration of a proposed measurement concept. The test cases use perfect and noisy artificial measurement data. The direct problem is solved by a finite difference method, which was an elementary step of the inverse solution. As the inverse solution is ill-posed, it is nearly impossible to get reliable final results based on one genetic run (inverse solution). We propose making a '*map*' of the environment of the global optimum of every searched parameter. Using the map the global optimum can easily be estimated in a very reliable and accurate way. The results show very good agreement even for the case of noisy data between the original material properties (global optimum) and the ones determined by the proposed evaluation method (estimated global optimum). In this way, the proposed method has very good potential in being used with real measurement data. Moreover, the presented genetic algorithm can be an effective tool in a great variety of inverse heat conduction problems.

**Keywords** Finite difference method · Genetic algorithm · Inverse heat conduction · Thermal conductivity · Volumetric heat capacity

B. Czél (✉) · Gy. Gróf
Department of Energy Engineering, Budapest University of Technology and Economics,
Műegyetem rkp. 3, Budapest 1111, Hungary
e-mail: czel@energia.bme.hu

## 1 Introduction

The thermal conductivity and volumetric heat capacity are the major material properties in transient heat conduction phenomena. Knowledge of these properties is always needed in solving technical problems connected to heat conduction. These two material properties are generally not independent of temperature, and in most cases, the character of their temperature dependence is unknown. The application of materials with strongly temperature-dependent properties has been increasing (polymers, composites, foams, etc.) due to the continuous development of material technology.

The subject of the actual research work is development of a measurement technique and an evaluation method for determination of the temperature-dependent thermal conductivity and volumetric heat capacity that is characterized by the need of a single transient measurement. The technique proposed in this article may simplify the commonly used measurement methods where the characterization of the temperature dependence of thermophysical properties needs time-consuming measurements at every temperature span $\Delta T$. To achieve our aim, the measurement and evaluation should be matched and this process means several modifications on both sides.

The aim of this article is the presentation of three test cases of the evaluation method, and proving that the proposed method has very good potential in being applied to real measurement results. The test cases were defined considering the proposed measurement technique.

The thermophysical properties of a material are usually determined using results of some kind of temperature measurement. In this way, we have the output data (containing measurement errors) of the heat conduction equation, and we need some of the input parameters. This is an inverse heat conduction problem (IHCP). There are several methods for solving such types of inverse problems [1,2], but none of them is generally accepted. The IHCP is an intensively researched field of thermal sciences.

We can find many different methods among the classical approaches. Yang [3] used a sequential method and a modified Newton–Raphson method for estimation of the boundary conditions in a two-dimensional (2D) nonlinear IHCP. Zmywaczyk [4] applied the modified Newton–Raphson method to determine temperature-dependent thermophysical properties ($k_r$, $k_z$, $\rho c_p$) of an orthotropic material. Del Barrio [5] identified heat sources in a 2D diffusion problem by the Lagrange theory. Pohanka et al. [6] applied the simplex method to determine the temperature-dependent thermal properties ($k$, $\rho c_p$) of a fused silica shell. Chiwiacowsky and Campos Velho [7] compared a non-classical (genetic algorithm) method with two classical methods (conjugate gradient method and a quasi-Newton method) through the estimation of the initial condition of a 1D slab.

The application of artificial-intelligence-based methods and evolutionary algorithms to an IHCP has been spreading as a result of the rapid development of computer science and technology. There are two main methods: neural networks and genetic algorithms. Raudensky et al. [8] determined the boundary conditions and time constant of a temperature sensor based on temperature readings from the sensor by a neural network. Shiguemori et al. [9] following the work of Krejsa et al. [10] studied two different neural networks (multilayer perceptron and radial base function) to estimate the heat flux versus time function as a boundary condition of a 1D slab. Deng and

Hwang [11] applied the back propagation neural network to estimate the boundary condition in 1D and 2D cases of IHCP.

The genetic algorithms (GA) work similarly to the biological evolution of nature [12,13]. The GAs are mostly said to be optimization methods searching for the best solution of an ill-posed problem. The searching process is controlled by the objective function. The GAs can work with a lot of unknown variables and have the ability to find the global optimum of a problem. This makes genetic algorithms applicable for the solution of IHCPs. Raudensky et al. [14] determined the heat transfer coefficient history of a 1D slab using GA. Woodbury [15] used GA for the estimation of the surface heat flux history of a 1D slab. Chiwiacowsky et al. [16] applied parallel GA to determine the initial condition of an insulated 1D slab. Garcia [17] elaborated an extended elitist GA algorithm to estimate simultaneously the orthotropic thermal conductivity $k_x, k_y$ and volumetric heat capacity $\rho c_p$ from experimental temperature histories and known heat flux with respect to a composite material. Zmywaczyk [18] proposed a hybrid method of differential evolution (DE), described primarily by Price and Storn in [19], later on developed in [20], and the Levenberg–Marquardt algorithm for simultaneous estimation of temperature-dependent thermophysical parameters ($k_r$, $k_z$, $\rho c_p$).

## 2 Problem-Solving Method

The prior determination of the measurement concept has to be the first step in development of the evaluation method. A sample in the form of a hollow cylinder with an inside core and an outer shield is a generally applied arrangement used to determine its thermophysical properties. In steady-state conditions the thermal conductivity is determined by the measured temperature difference between the core and the shield. This arrangement can be applied in the case of transient measurements as well. The advantage of applying a cylindrical sample is that 1D heat conduction can be performed by properly applied boundary conditions. The measurement of the transient temperatures on the inner and outer surfaces of the sample is performed by thermocouples placed in the core and the shield (Fig. 1). While performing an experiment, the core-sample-shield system is heated to a predefined homogeneous temperature and next it is cooled by forced air flow during which the transient temperatures on the inner and outer surfaces of the sample (Fig. 1) are recorded (one step cooling down).

The evaluation method means determination of the temperature-dependent material properties from the measured transient temperature data. In order to solve this inverse problem by a GA we have to solve the transient heat conduction problem in the core-sample-shield cylindrical system (*direct problem*) which is an elementary step of the GA. The essence of the inverse solution is to find the set of thermophysical parameters when the fit of the calculated transient temperatures is in agreement with the measured ones.

In this article, we present three test cases of the evaluation method with perfect and noisy artificial measurement data. The test cases were defined according to the proposed measurement concept. In all test cases we have to find the temperature-dependent thermal conductivity and volumetric heat capacity from the artificial

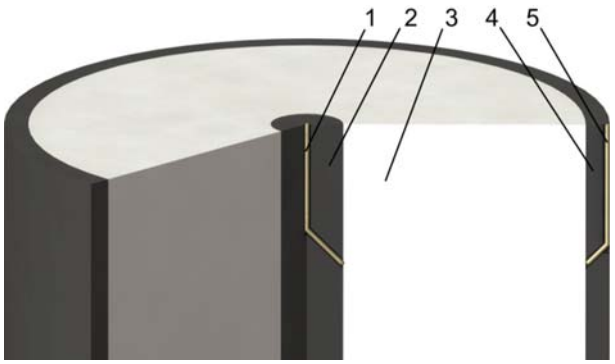


**Fig. 1** Proposed measurement arrangement (*1* thermocouple in the core, *2* core, *3* sample, *4* shield, *5* thermocouple in the shield)

measurement data. In two cases the artificial measurements have no errors; in the third case they have random error with the specified magnitude.

## 3 Solution of the Direct Problem

The *direct solution* means determination of the transient temperature field of the cylindrical system formed by three layers (see Fig. 1) with temperature-dependent thermophysical properties. The task is to solve the 1D partial differential equation of the heat conduction written in a cylindrical coordinate system for the case of temperature-dependent material properties. On the outer surface of the three-layer cylindrical system, the boundary condition of the 3rd kind (heat convection) is considered. A homogeneous initial temperature distribution at time $t = 0$ is assumed. The equation of energy conservation has the following form:

$$\rho c_p(T)\frac{\partial T}{\partial t} = k(T)\frac{\partial^2 T}{\partial r^2} + \frac{\partial k(T)}{\partial T}\left(\frac{\partial T}{\partial r}\right)^2 + \frac{1}{r}k(T)\frac{\partial T}{\partial r} \tag{1.1}$$

$$\left.\frac{\partial T}{\partial r}\right|_{r=0} = 0 \quad -k(T)\left.\frac{\partial T}{\partial r}\right|_{r=R} = h(T_R - T_\infty) \tag{1.2}$$

$$T(r, t=0) = T_0 \tag{1.3}$$

where $h$ is the heat transfer coefficient, $T_R$ is the temperature of the outer surface of the shield, and $T_\infty$ is the temperature of the forced air flow. The temperature-dependent thermal conductivity $k(T)$ and the volumetric heat capacity $\rho c_p(T)$ are assumed to be linear as follows:

$$\rho c_p(T) = a_1 T + a_0 \qquad k(T) = b_1 T + b_0 \tag{2}$$

Equation 1 is solved using the finite difference method, central differences for space, and the explicit Euler method for time integration. The finite difference form of Eq. 1 is as follows:

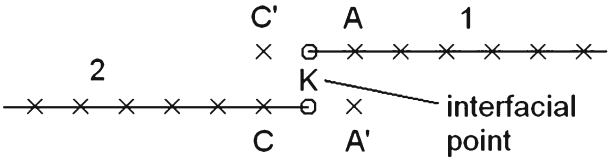


**Fig. 2** Finite difference grid at the interfaces of the layers

$$\left(a_1 T_{k,i} + a_0\right) \frac{T_{k+1,i} - T_{k,i}}{\Delta t} = \left(b_1 T_{k,i} + b_0\right) \frac{T_{k,i+1} - 2T_{k,i} + T_{k,i-1}}{\Delta r^2} + b_1 \frac{T_{k,i+1}^2 - 2T_{k,i+1}T_{k,i-1} + T_{k,i-1}^2}{4\Delta r^2} + \frac{1}{r_i}\left(b_1 T_{k,i} + b_0\right) \frac{T_{k,i+1} - T_{k,i-1}}{2\Delta r} \quad (3)$$

where the index $k$ refers to the time and the index $i$ refers to the space. Equation 3 is not applicable in special grid points. The points that need special treatment are located at the center of the cylinder ($r = 0$), on the interfaces of the layers ($r = R1, R2$) and at the outer surface of the cylinder ($r = R$).

The boundary condition applied on the interfaces of the layers ($r = R1, R2$) comes from the set of Eq. 4. Equations 4.1 and 4.2 represent the equation of energy conservation considering that the K interfacial point (Fig. 2) belongs to materials 1 and 2. Two virtual points ($T'_{\mathrm{A}}$ and $T'_{\mathrm{C}}$) also have to be considered. Equation 4.3 represents the equality of the heat fluxes. The two virtual points should be eliminated from the set of Eq. 4 to get the proper equation to be applied on the interfaces of the layers. The result is very complex and there is no room here to present it.

$$\rho c_{p1}(T) \frac{\partial T}{\partial t} = k_1(T) \frac{T_{\mathrm{A}} - 2T_{\mathrm{K}} + T'_{\mathrm{C}}}{\Delta r^2} + \frac{\partial k_1(T)}{\partial T} \frac{T_{\mathrm{A}}^2 - 2T_{\mathrm{A}}T'_{\mathrm{C}} + T_{\mathrm{C}}^{2\prime}}{4\Delta r^2} + k_1(T) \frac{T_{\mathrm{A}} - T'_{\mathrm{C}}}{2R_{\mathrm{K}}\Delta r} \quad (4.1)$$

$$\rho c_{p2}(T) \frac{\partial T}{\partial t} = k_2(T) \frac{T'_{\mathrm{A}} - 2T_{\mathrm{K}} + T_{\mathrm{C}}}{\Delta r^2} + \frac{\partial k_2(T)}{\partial T} \frac{T_{\mathrm{A}}^{2\prime} - 2T'_{\mathrm{A}}T_{\mathrm{C}} + T_{\mathrm{C}}^2}{4\Delta r^2} + k_2(T) \frac{T'_{\mathrm{A}} - T_{\mathrm{C}}}{2R_{\mathrm{K}}\Delta r} \quad (4.2)$$

$$k_2(T)\left(T'_{\mathrm{A}} - T_{\mathrm{C}}\right) = k_1(T)\left(T_{\mathrm{A}} - T'_{\mathrm{C}}\right) \quad (4.3)$$

The solution of the direct problem is an elementary step of the inverse solution, and because of this, it should be used many times. The reduction of the CPU time of the direct solution was an especially important challenge. To achieve this aim, we generated and tested different calculation versions using simplifications in the mathematical formulation. (Moreover, we solved Eq. 1 by the Crank–Nicolson method as well, but the explicit method proved to be more efficient [21].) Because of the simplifications used, we had to take care about the accuracy in addition to the reduction of the CPU time. We tested the effect of changing the stability coefficient and the grid refinement as well. The reference calculations were verified by analytical and finite-element (FE) calculations (more details in [21]). Finally we reduced the CPU time of one direct

calculation from 15.3 s to 0.7 s with an average absolute deviation of 0.097 °C when compared to the reference calculation values. For obtaining the results in this article, we used the explicit calculation version called Exp130 in [21]. The calculation of the direct solution is performed by a program written in the Matlab environment by the authors.

## 4 Solution of the Inverse Problem

The inverse solution of the boundary-value problem means in this case determination of the temperature-dependent thermal conductivity and volumetric heat capacity from the artificial measurement data. We intend to measure the transient temperature at the inner and outer surfaces of the sample (Fig. 1) during a cooling process. According to this, the artificial measurement data means the temperature versus time history of the cooling process at the two interfacial points mentioned above. The artificial measurement data are generated using the result of a direct solution. This way we know the accurate material properties that we are searching with the algorithm, and we can compare the accurate properties with the ones found by the algorithm.

The IHCPs belong to the ill-posed boundary-value problems. The genetic algorithms have been successfully applied in solving such a kind of problems. Genetic means that the algorithm tries to model the biological evolution. The "search space" contains the solutions of the problem. The algorithm is working in parallel on a number of candidates of the solution. The possible solutions are called *entities.* The entities can be optimal, less optimal, or unacceptable. A certain group of entities forms the *population.* During the evolution of the population, further and further *generations* are created. The entities (solutions of the problem) are coded into a data structure, and the algorithm applies different *genetic operators* on this data structure. The operators are similar to the biological descent keeping the valuable information. The genetic algorithm assures survival and spreading of the best entities in the new generation. The key issue of the genetic algorithms is the selection and coding of the major characteristics of the problem (*representation)*, and moreover, the selection of the proper *objective function* that is used for ranking the entities.

The task of the genetic algorithm is to find the entities (sets of material properties) when best matching exists among the measured (artificial in this case) and calculated transient temperature data. For better understanding of the algorithm structure, see Fig. 3. The temperature dependence of the material properties is considered to be linear. This way we want to determine four parameters $(a_0, a_1, b_0, b_1)$ according to Eq. 2. It means that one entity $(e)$ is characterized by four parameters:

$$e = [a_0, a_1, b_0, b_1] \tag{5}$$

The parameter values are picked up from a given range. The population consists of 30 entities and the first generation is formed randomly—(*Step 1* in Fig. 3). The objective function $E$ (Eq. 6) is based on the absolute discrepancy between the artificial measurement and the calculated transient temperature data. To calculate the objective function, the direct problem has to be solved for every entity—(*Step 2* in Fig. 3). The

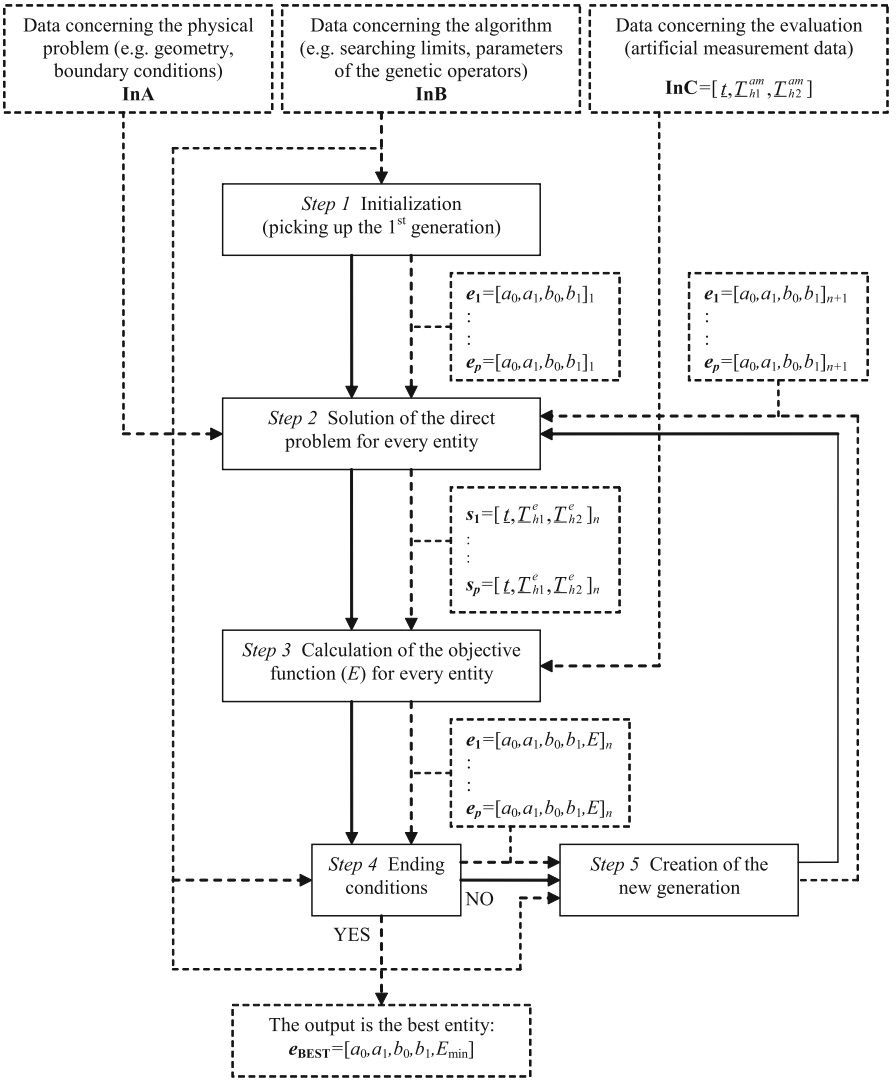


**Fig. 3** Structure of the applied genetic algorithm

objective function is then calculated as the sum of the absolute discrepancies in 100 time steps for the inner surface and in 100 time steps for the outer surface of the sample as follows:

$$E = \sum_{i=1}^{100} \left| T_{i,h1}^{\mathrm{e}} - T_{i,h1}^{\mathrm{am}} \right| + \sum_{i=1}^{100} \left| T_{i,h2}^{\mathrm{e}} - T_{i,h2}^{\mathrm{am}} \right| \tag{6}$$

where the index $h1$ refers to the inner surface, and $h2$ refers to the outer surface of the sample, the index $i$ refers to different time steps, $e$ refers to the temperature results

of the actual entity, and the index *am* refers to the artificial measurement data. The absolute discrepancy was chosen as the objective function instead of the commonly used squared errors, because we think that the absolute discrepancy is more expressive and easier to understand. The applied GA uses rank selection, so we need only the rank of the entities. In this way, the absolute value of the objective function does not have an effect on the algorithm.

Reasons for using 100 time steps:

- We think that it is sufficient to calculate the difference between two non-periodical curves.
- Usually one direct calculation has about 10,000 to 50,000 time steps. Using only 100 time steps in the objective function, we do not have to treat such big vectors in the GA, and the algorithm runs faster.
- The direct calculation needs different number of time steps depending on the tested material. (The direct calculation usually ends when the dimensionless temperature is about 0.05.) With a predefined number of time steps in the objective function, its scale is the same in all cases.

During the evaluation process the values of the objective function are calculated for every entity and they are ranked into increasing series (the minimum is the best)—(*Step 3* in Fig. 3). Termination of the algorithm happens if the previously defined number of the generation has been reached or the objective function has reached its preset limit (*Step 4* in Fig. 3). If the requirements of the termination are not met, a new generation is born (*Step 5* in Fig. 3). In the process of generating the new generation the best entity remains in the original form (elitism). Four entities are generated from the best one by *creep* or *mutation*. Creep means multiplying all parameters by a number randomly selected from the range of $(1-crp, 1+crp)$, where *crp* is a previously defined number between 0 and 1 [12,15]. Mutation means changing a randomly selected parameter with a new one picked up randomly from a given range. This range is determined as in the case of creep. Fifteen entities are generated applying the usual reproduction method: *selection*, *crossover*, and mutation or creep. The "parents" are selected randomly from a previously defined number of the best entities. During crossover the randomly selected proper parameters of two parents are exchanged. There is a threshold for mutation and creep, which means that every entity has a previously defined chance to mutate and creep. The last 10 entities are generated similarly to the first generation to favor the finding of the global optimum of the solution. Applying the genetic operators, care had to be taken to the fact that the parameters are not independent from each other ($a_1$ depends on the value of $a_0$, and $b_1$ depends on the value of $b_0$). The calculation of the inverse solution is performed by a program written in the Matlab environment by the authors.

In Fig. 3, the boxes with continuous edges show the steps of the algorithm, the continuous lines between these boxes show the process of the algorithm, the dashed lines show the way of information, the dashed border boxes show the type of information, the index $p$ refers to the number of the entity in the population, the index $n$ refers to the number of the generations, bold letters refer to a data set of variables of a different kind, and underlined letters refer to a data set of variables of the same kind. In Fig. 3,

one can find the type of input and output data for the algorithm itself and also for all steps of the algorithm.

## 5 Results

Here, we present the results of three test cases of the evaluation method using artificial measurement data in it. For all test cases we wanted to determine the temperature-dependent thermal conductivity and volumetric heat capacity, which means there were four unknown parameters to be estimated according to the method described in Sect. 4. In all test cases we used the same initial and boundary conditions, and the material properties of the core and shield were also assumed to be the same. The thermophysical properties of the core and the shield were similar to those for stainless steel (according to our plans about the real measurement equipment). The thermophysical properties of the core and shield were considered to be constant because the result of the set of Eq. 4 became much simpler and the CPU time of one direct calculation became shorter. Otherwise, consideration of a realistic temperature dependence for the case of the core and shield has a slight effect on the examined transient temperature curves. In Test Case 1, the material properties of the sample used were those for polytetrafluoroethylene (PTFE). In Test Case 2, we used the same sample material properties at 0 °C as in Test Case 2, but the gradient of the temperature dependence was increased. In both Test Cases 1 and 2, the artificial measurement data had no errors. In Test Case 3, the sample material properties were the same as in Test Case 2, but random measurement errors over the range [−0.5 °C, +0.5 °C] were added to the artificial measurement data. The parameter values of the test cases can be found in Table 1, where a.m. refers to the artificial measurement data, $T_0$ refers to the initial temperature, $T_\infty$ refers to the ambient temperature, $h$ refers to the heat transfer coefficient, $R$ refers to the outer

**Table 1** Parameters of the three test cases

| | Core and shield | Sample | | Sample | | Sample | | |
|---|---|---|---|---|---|---|---|---|
| | | Test Case 1 | | Test Case 2 | | Test Case 3 | | |
| | Constant | 0 °C | 200 °C | 0 °C | 200 °C | 0 °C | 200 °C | |
| $k$ | 18 | 0.24 | 0.204 | 0.24 | 0.18 | 0.24 | 0.18 | $(W \cdot m^{-1} \cdot K^{-1})$ |
| $c$ | 460 | 1833 | 1980 | 1833 | 2367 | 1833 | 2367 | $(J \cdot kg^{-1} \cdot K^{-1})$ |
| $\rho$ | 7800 | 1200 | 1200 | 1200 | 1200 | 1200 | 1200 | $(kg \cdot m^{-3})$ |
| a.m. | | Perfect | | Perfect | | Noisy | | |
| $T_0$ | 200 | | | | | | | (°C) |
| $T_\infty$ | 20 | | | | | | | (°C) |
| $h$ | 47.6 | | | | | | | $(W \cdot m^{-2} \cdot K^{-1})$ |
| $R$ | 25 | | | | | | | (mm) |
| $R_1$ | 3 | | | | | | | (mm) |
| $R_2$ | 23 | | | | | | | (mm) |
| $g$ | 26 | | | | | | | |

**Table 2** Parameters of the genetic runs

| | Test Case 1 | | Test Cases 2 and 3 | | |
|---|---|---|---|---|---|
| | Min | Max | Min | Max | |
| $a_0$ | 2 | 3 | 2 | 3 | $(\mathrm{MJ \cdot m^{-3} \cdot K^{-1}})$ |
| $a_1$ | −35 | 35 | −50 | 50 | (%) |
| $b_0$ | 0.1 | 0.5 | 0.1 | 0.5 | $(\mathrm{W \cdot m^{-1} \cdot K^{-1}})$ |
| $b_1$ | −35 | 35 | −50 | 50 | (%) |
| Max. number of generations | 200 | | | | |
| Limit of the objective function | 5 | | | | (°C) |
| Number of parents | 15 | | | | |
| Mutation chance | 50 | | | | (%) |
| Creep chance | 50 | | | | (%) |
| Creep coefficient | 0.05 | | | | |

radius of the shield, $R1$ refers to the inner radius of the sample, $R2$ refers to the outer radius of the sample, and $g$ refers to the number of grid points. The assumed temperature dependencies of the sample material properties were given in Eq. 2. The value of the heat transfer coefficient was determined as a result of a measurement performed by the proposed equipment with a copper reference sample. The heat transfer coefficient was evaluated using a lumped thermal capacity model.

In all test cases we used the same parameters for the genetic operators and the same ending conditions. The algorithm terminates after 200 generations in the test cases or when the objective function is below a defined limit (5 °C in the test cases). The searching limits of the parameters are a bit different in the three test cases because of the different sample material properties. The searching limit for the $a_1$ and $b_1$ parameters is defined in percentage. This means the percentage deviation between the material property at the point of the maximum temperature and at 0 °C, respectively. For example, the thermal conductivity at the maximum temperature in Test Case 1 cannot be higher than $0.5\,\mathrm{W \cdot m^{-1} \cdot K^{-1}} + 35\,\% = 0.675\,\mathrm{W \cdot m^{-1} \cdot K^{-1}}$. The parameters of the genetic operators, ending conditions, and searching limits can be found in Table 2.

In Fig. 4, a convergence diagram of 10 genetic runs is presented. The objective function value of the best entity of the actual generation is plotted as a function of the number of generations (Test Case 1). In some cases the convergence gets very slow after some generations, and sometimes the objective function value is continuously decreasing. The algorithm has the ability to step out from a local minimum area of the objective function to a better one as the continuous grey curve shows in Fig. 4.

In the genetic algorithm there are a lot of random operations. In this way, the algorithm always stops with a different objective function value ($E$) and parameter set ($e$). Our experience was that there is no definite relation between the objective function value and the accuracy of the estimation of the material parameters in $e$. It is because the inverse solution is ill-posed. It is nearly impossible to get reliable final results based on one genetic run. We propose making a "*map*" of the environment of the global optimum of every searched parameter. Using the map, the global optimum can

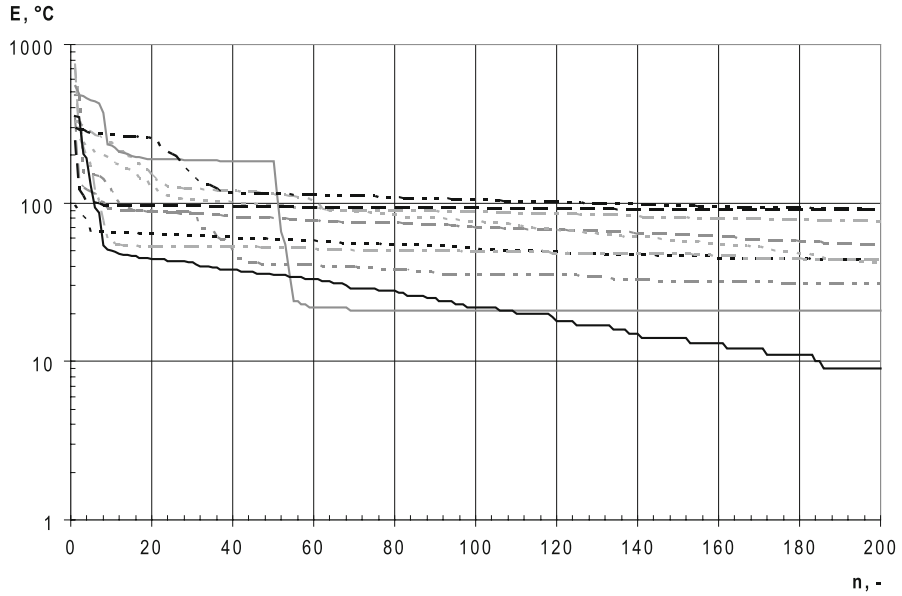


**Fig. 4** Convergence diagram of 10 genetic runs with the same parameters (Test case 1)

easily be estimated in a very reliable and accurate way. To create the map, we use the results of 100 independent genetic runs (inverse solutions) with the same settings in all test cases. The creation of the map and the estimation method of the global optimum are described below.

### 5.1 Results of Test Case 1

In Fig. 5a–d, the results of 100 independent genetic runs are shown. Every point in the diagrams comes from the best entity of the last generation of a run. We plot the volumetric heat capacity and the thermal conductivity at 0 °C and at 200 °C as a function of the objective function value of the entity under consideration. (In Fig. 5a, c the $a_0$ and $b_0$ parameters of the genetic algorithm are plotted, respectively, but in Fig. 5b, d, the results are calculated from the $a_1$ and $b_1$ parameters of the genetic algorithm, respectively, for better understanding of the results.) An entity has a data point in all four—a, b, c, and d—diagrams. For example, a point at $E = 128$ °C can be found in all four diagrams, and these points belong to the same entity. The horizontal line on the diagrams means the original material property what we wanted to find (global optimum).

The results in Fig. 5a–d clearly show that the material properties found by the genetic algorithm converge to the original ones if the objective function values are decreasing. Lower- and upper-limit curves can be found for all four diagrams, and these limit curves intersect each other nearly perfectly at the original material property. In this case, these limit curves are quite symmetric to the original property and are nearly linear. There are a lot of results inside these limit curves. For example in Fig. 5c we can find an entity very close to the original material property with an objective

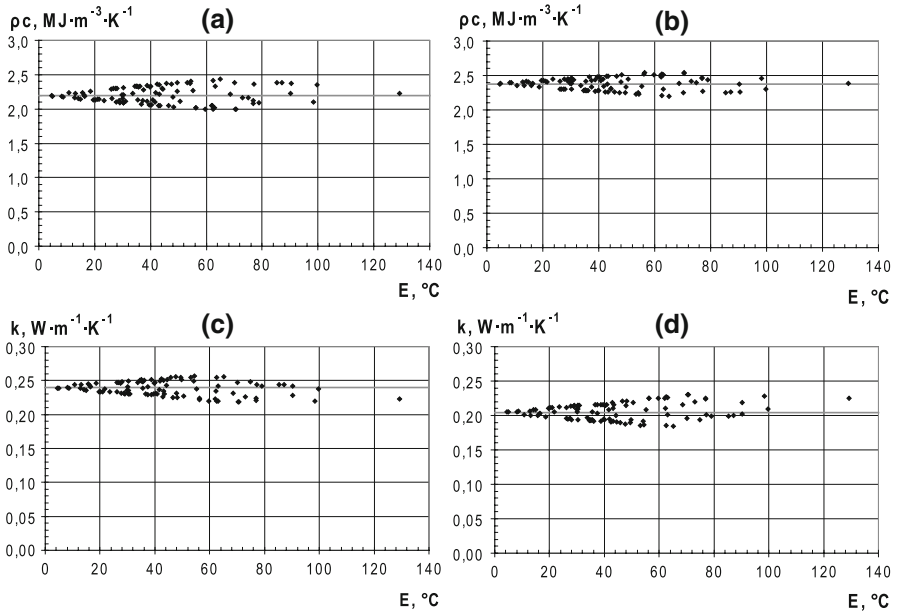


**Fig. 5** Results of Test Case 1. (**a**) $\rho c$ at 0 °C, (**b**) $\rho c$ at 200 °C, (**c**) $k$ at 0 °C, and (**d**) $k$ at 200 °C

function value of about 100 °C. We can find this entity in the other diagrams as well (the point with the same objective function value). If we check this entity in Fig. 5a, b, we can see that it is quite far from the original property and the tendency of the temperature dependence is the opposite of the searched one (in Fig. 5a the value of this entity is higher than in Fig. 5b). This is because we have quite a high value for the objective function (as the objective function value is determined by all parameters of one entity).

## 5.2 Results of Test Case 2

The results of Test Case 2 can be found in Fig. 6a–d. The method of plotting the results is the same as in Test Case 1. In Test Case 2, the gradient of the temperature dependence of both material properties is higher than in Test Case 1. We obtained consistent results to the original material properties for both the material properties at both the temperature levels. Similar to Test Case 1, lower- and upper-limit curves can also be found here in all four diagrams and these curves also tend to intersect each other at the original material property. The lower-limit curve in Fig. 6a is affected by the searching limit of the $a_0$ parameter. In Fig. 6b, the upper-limit curve also looks like it has a limit of $3\,\mathrm{MJ}\cdot\mathrm{m}^{-3}\cdot\mathrm{K}^{-1}$, but it is also the effect of reaching the lower limit of the $a_0$ parameter as the upper limit at 200 °C was $3\,\mathrm{MJ}\cdot\mathrm{m}^{-3}\cdot\mathrm{K}^{-1}+50\,\%$. Besides this, the upper- and lower-limit curves tend to be linear (before reaching the parameter limits), but unlike Test Case 1, these are not symmetrical with the original material property value just below the objective function value of 20 °C. In Test Case 2, there are also some results inside the limit curves; the explanation is the same as in Test Case 1.

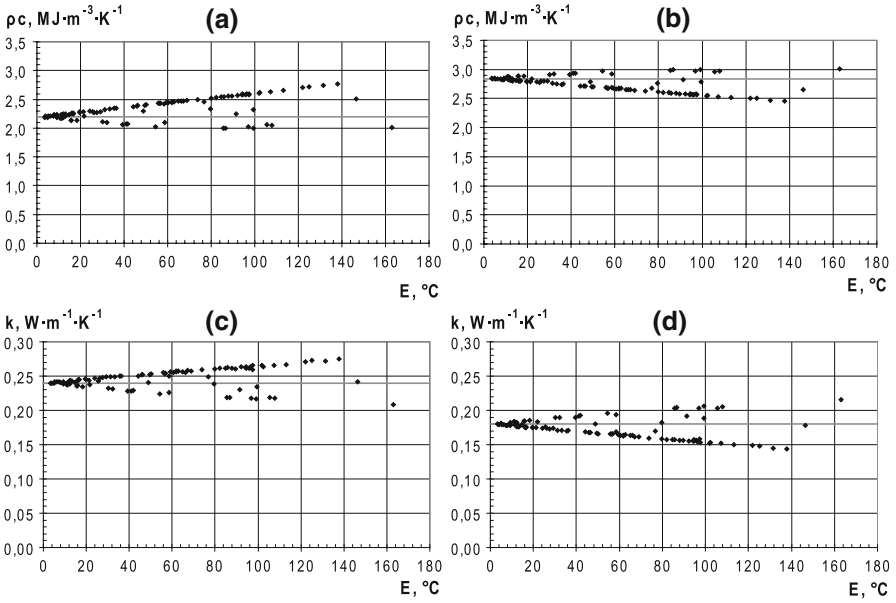


**Fig. 6** Results of Test Case 2. (**a**) $\rho c$ at 0 °C, (**b**) $\rho c$ at 200 °C, (**c**) $k$ at 0 °C, and (**d**) $k$ at 200 °C

### 5.3 Results of Test Case 3

In Test Case 3, the artificial measurement data were noisy and the original material properties were the same as in Test Case 2. We added a random error to the perfect artificial measurement data from the range of [−0.5 °C, 0.5 °C]. The objective function value can be calculated between the perfect and noisy artificial measurement data. Theoretically this value is 50 °C (as we have 200 temperature data points), and in this specific case it is 48.96 °C. This means that the objective function value during the genetic runs should converge to 48.96 °C instead of 0 °C like in the case of perfect artificial measurement data (Test Cases 1 and 2).

The results of Test Case 3 can be followed in Fig. 7a–d. The method of plotting the results is the same as in Test Cases 1 and 2. The results clearly converge to the original material properties at the objective function value of about 50 °C. The results are quite similar to the results of Test Cases 1 and 2. There are also lower and upper-limit curves in all four diagrams. These curves are also close to linear but not so clearly as in Test Case 1 or 2. The results are quite symmetric to the original material property value in all four diagrams below the objective function value of 60 °C.

### 5.4 Estimation Method of the Global Optimum

Using this evaluation method for real measurements, we do not know the original material properties. We have to select or calculate the final material properties (estimated global optimum) from the results of a set of genetic runs. The first is plotting the results like Figs. 5, 6, and 7. After that we propose two possible ways:

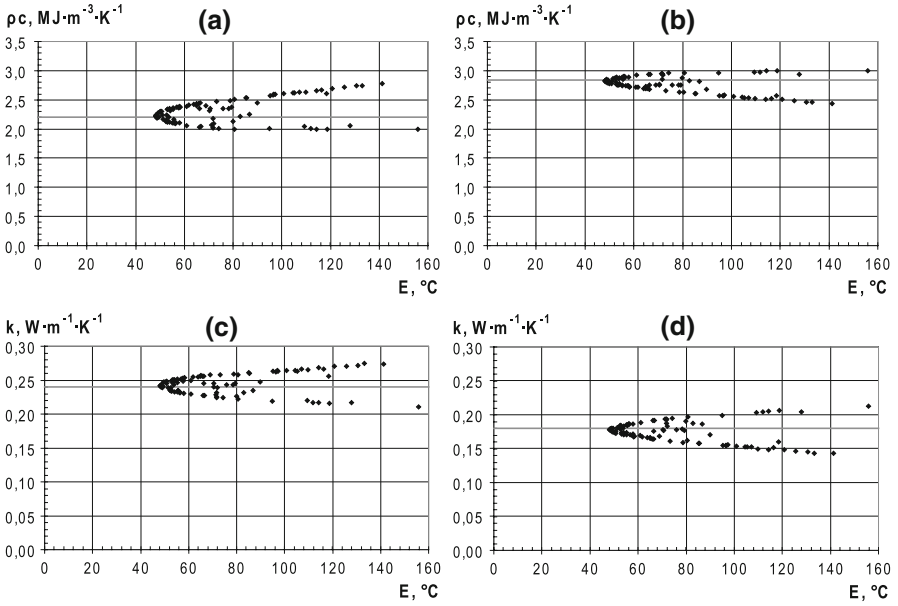


**Fig. 7** Results of Test Case 3. (**a**) $\rho c$ at 0 °C, (**b**) $\rho c$ at 200 °C, (**c**) $k$ at 0 °C, and (**d**) $k$ at 200 °C

(a) We can choose the entity with the lowest objective function value if the results clearly show lower- and upper-limit curves and these tend to intersect each other close to this entity.

(b) The results usually tend to be symmetric with the original value (global optimum) below a limit of the objective function. We have to select this limit and simply calculate the average of the resulting material properties with an objective function value below this limit.

If we need to be sure, we can apply both methods and compare the results. The comparison of the original (global optimum) and final material properties (estimated global optimum) gained using both the proposed methods for Test Cases 1, 2, and 3 is given in Table 3. In most cases choosing the best entity gives the better result than the average calculation, but the difference is not too significant. Choosing the best entity gives less than 0.4 % deviation in the case of both material properties and both temperature levels when compared to the original ones in Test Cases 1 and 2, which means very good accuracy for the case of perfect artificial measurement data. In Test Case 3, choosing the best entity as a final result has a maximum percentage deviation of 1.22 % when compared to the original material properties. This is also a very good result considering the noisy artificial measurement data.

It should be mentioned that the determined material properties can be applied only in the 20 °C to 200 °C temperature range, because the cooling process starts at 200 °C and ends at 20 °C in the proposed measurement equipment.

In Fig. 8a–c the final results of Test Case 3 are presented using the best entity. In Fig. 8a, the temperature versus time history calculated with the material properties of the final result of Test Case 3 and the applied artificial measurement data are shown.

**Table 3** Final material properties of Test Cases 1,2, and 3

| | Material properties | | | | Deviation from the original | | | |
|---|---|---|---|---|---|---|---|---|
| | $\rho c(0\,^\circ\mathrm{C})$ $(\mathrm{MJ}\cdot\mathrm{m}^{-3}\cdot\mathrm{K}^{-1})$ | $\rho c(200\,^\circ\mathrm{C})$ $(\mathrm{MJ}\cdot\mathrm{m}^{-3}\cdot\mathrm{K}^{-1})$ | $k(0\,^\circ\mathrm{C})$ $(\mathrm{W}\cdot\mathrm{m}^{-1}\cdot\mathrm{K}^{-1})$ | $k(200\,^\circ\mathrm{C})$ $(\mathrm{W}\cdot\mathrm{m}^{-1}\cdot\mathrm{K}^{-1})$ | $\rho c(0\,^\circ\mathrm{C})$ (%) | $\rho c(200\,^\circ\mathrm{C})$ (%) | $k(0\,^\circ\mathrm{C})$ (%) | $k(200\,^\circ\mathrm{C})$ (%) |
| **Test Case 1** | | | | | | | | |
| *original* | 2.200 | 2.376 | 0.24 | 0.204 | – | – | – | – |
| average $E < 40\,^\circ\mathrm{C}$ | 2.196 | 2.380 | 0.2393 | 0.2049 | −0.19 | 0.18 | −0.29 | 0.44 |
| best entity | 2.198 | 2.377 | 0.2392 | 0.2048 | −0.09 | 0.05 | −0.33 | 0.39 |
| **Test Case 2** | | | | | | | | |
| *original* | 2.200 | 2.840 | 0.24 | 0.18 | – | – | – | – |
| average $E < 20\,^\circ\mathrm{C}$ | 2.212 | 2.833 | 0.2408 | 0.1794 | 0.56 | −0.23 | 0.34 | −0.31 |
| best entity | 2.198 | 2.848 | 0.2396 | 0.1806 | −0.09 | 0.27 | −0.17 | 0.33 |
| **Test Case 3** | | | | | | | | |
| *original* | 2.200 | 2.840 | 0.24 | 0.18 | – | – | – | – |
| average $E < 60\,^\circ\mathrm{C}$ | 2.235 | 2.818 | 0.2421 | 0.1778 | 1.57 | −0.79 | 0.88 | −1.22 |
| best entity | 2.223 | 2.822 | 0.2416 | 0.1778 | 1.03 | −0.65 | 0.67 | −1.22 |

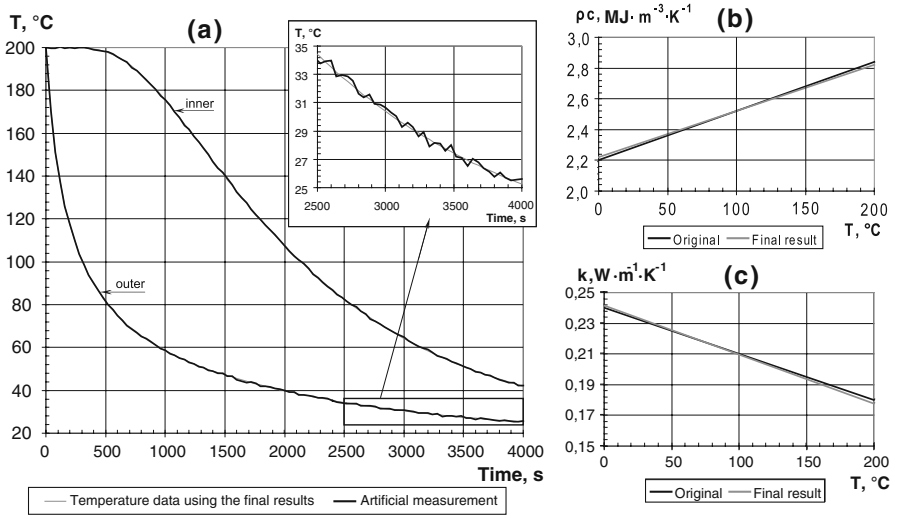


**Fig. 8** Final results of Test Case 3 using the best entity

The agreement between the curves is so good that we had to enlarge a part of it to show the different curves. In Fig. 8b, c the original and the final material properties of Test Case 3 are shown as a function of the temperature. There is very good agreement between the curves for the case of both material properties.

## 6 Conclusion

We tested a new genetic-algorithm-based evaluation method for simultaneous determination of the temperature-dependent thermal conductivity and volumetric heat capacity from transient temperature measurement data at two points according to the cooling process of a three-layered infinite cylinder. Three test cases were presented which were defined considering our proposed measurement concept. We used perfect artificial measurement data for Test Cases 1 and 2, and noisy artificial measurement data for Test Case 3. The direct problem was solved by the finite difference method, which was an elementary step of the inverse solution.

As the inverse solution is ill-posed, it is nearly impossible to get reliable final results based on one genetic run (inverse solution). We propose making a "*map*" of the environment of the global optimum of every searched parameter. Using the map the global optimum can easily be estimated in a very reliable and accurate way.

To create the map we used the results of 100 independent genetic runs with the same settings in all test cases. Plotting the searched material properties as a function of the objective function value of the GA, lower- and upper-limit curves could be found in all test cases and for all material properties. The lower- and upper-limit curves tend to intersect each other at the original material property (global optimum), which proves the convergence of the algorithm. For the determination of the final material properties (estimated global optimum), we proposed two methods: selection of the best entity

and/or the average method. In the test cases with perfect artificial measurement data, the best entity method had less than 0.4 % deviation for the case of both material properties and both temperature levels when compared to the original ones. In Test Case 3 with noisy artificial measurement data, the maximum percentage deviation was 1.22 when compared to the original properties. These results prove that the presented evaluation method works very well even with noisy temperature data and in this way it has very good potential in using it with real measurement data. Moreover, the presented genetic algorithm can be an effective tool in a great variety of IHCPs.

## References


1. J.V. Beck, B. Blackwell, C.R. St. Clair, *Inverse Heat Conduction: Ill-Posed Problems* (Wiley, New York, 1985)
2. M.N. Ozisik, H.R.B. Orlande, *Inverse Heat Transfer: Fundamentals and Applications* (Taylor & Francis, New York, 2000)
3. C. Yang, J. Thermophys. Heat Transfer **17**, 389 (2003)
4. J. Zmywaczyk, Arch. Thermodyn. **27**, 1 (2006)
5. E.P. Del Barrio, Inverse Probl. Eng. **11**, 515 (2003)
6. M. Pohanka, K.A Woodbury, J. Woolley, in *Proceedings IMECE 2002 International Mechanical Engineering Congress and Exposition*, New Orleans (2002)
7. L.D. Chiwiacowsky, H.F. Campos Velho, Inverse Probl. Eng. **11**, 471 (2003)
8. M. Raudensky, J. Horsky, J Krejsa, Int. Commun. Heat Mass Transfer **22**, 661 (1995)
9. E.H. Shiguemori, F.P. Harter, H.F. Campos Velho, J.D.S. da Silva, Tend. Math. Apl. Comput. **3**, 189 (2002)
10. J. Krejsa, K.A. Woodbury, J.D. Ratliff, M. Raudensky, Inverse Probl. Eng. **7**, 197 (1999)
11. S. Deng, Y. Hwang, Int. J. Heat Mass Transfer **49**, 4732 (2006)
12. L. Davis, *Handbook of Genetic Algorithms* (Van Nostrand Reinhold, New York, 1991)
13. M. Mitchell, *An Introduction to Genetic Algorithms* (The MIT Press, Cambridge, 1996)
14. M. Raudensky, K.A. Woodbury, J. Kral, T. Brezina, Numer. Heat Transfer B **28**, 293 (1995)
15. K.A. Woodbury, in *Proceedings 4th International Conference on Inverse Problems in Engineering*. Angra dos Reis, Brazil (2002)
16. L.D. Chiwiacowsky, H.F. Campos Velho, A.J. Preto, S. Stephany, in *Proceedings XXIV Iberian Latin-american Congress on Computational Methods in Engineering (CILAMCE-2003)*, Ouro Preto (MG), Brazil (2003)
17. S. Garcia, Experimental design optimization and thermophysical parameter estimation of composite materials using genetic algorithms, Ph.D. thesis (1999). http://scholar.lib.vt.edu/theses/available/etd-061899-095435/unrestricted/etd.pdf
18. J. Zmywaczyk, Arch. Thermodyn. **28**, 89 (2007)
19. R. Storn, K. Price, Differential evolution—a simple and efficient adaptive scheme for global optimization over continuous spaces, Technical Report TR-95-012, ICSI (1995). www.icsi.berkeley.edu/~storn/
20. K.V. Price, R.M. Storn, J.A. Lampinen, *Differential evolution: a practical approach to global optimization* (Springer, Berlin, Heidelberg, 2005)
21. B. Czél, Gy. Gróf, in *Proceedings CHT-08 ICHMT International Symposium on Advances in Computational Heat Transfer*, Marrakech, Morocco (2008)